Umar et al. Egyptian Journal of Medical Human Genetics (2020) 21:67
https://doi.org/10.1186/s43042-020-00111-2

Egyptian Journal of Medical Human Genetics

RESEARCH Open Access

Computational evaluation of potent 2-(1H-imidazol-2-yl) pyridine derivatives as potential *V600E-BRAF* inhibitors

Abdullahi Bello Umar*, Adamu Uzairu, Gideon Adamu Shallangwa and Sani Uba

Abstract

Background: *V600E-BRAF* is a major protein target involved in various types of human cancers. However, the acquired resistance of the *V600E-BRAF* kinase to the vemurafenib and the side effects of other identified drugs initiate the search for efficient inhibitors. In the current paper, virtual docking screening combined with drug likeness and ADMET properties predictions were jointly applied to evaluate potent 2-(1H-imidazol-2-yl) pyridines as *V600E-BRAF* kinase inhibitors.

Results: Most of the studied compounds showed better docking scores and favorable interactions with the*iV600E-BRAF* target. Among the screened compounds, the two most potent (14 and 30) with good rerank scores (−124.079 and −122.290) emerged as the most effective, and potent *V600E-BRAF* kinase inhibitors which performed better than vemurafenib (−116.174), an approved *V600E-BRAF* kinase inhibitor. Thus, the docking studies exhibited that these compounds have shown competing inhibition of *V600E-BRAF* kinase with vemurafenib at the active site and revealed better pharmacological properties based on Lipinski's and Veber's drug-likeness rules for oral bioavailability and ADMET properties.

Conclusion: The docking result, drug-likeness rules, and ADMET parameters identified compounds (14 and 30) as the best hits against *V600E-BRAF* kinase with better pharmacological properties. This suggests that these compounds may be developed as potent V600E-BRAF inhibitors.

Keywords: Pyridine derivatives, *V600E-BRAF*, Molecular docking, ADMET

Background

The anomalous activation of *RAF*, commonly *BRAF*, is responsible for the amplification of the *MAPK* pathway and is often observed in cancers and also contributes to the oncogenesis [1]. Pathological studies revealed that the activated forms of the *BRAF* target is present in about 8% of all human cancers [2] and are often connected with melanoma (66%) [3]. What is important is that 90% of the observed *BRAF* mutations are that of *V600E*, which intensifies the kinase activity, and incidentally stimulates the signaling at notable high levels [4]. In this regard, *V600E-BRAF* kinase has been a target of concern for therapeutic intervention targeting which has verified to be the main success in the area of melanoma therapeutics. For example, vemurafenib (PLX4032) was clinically approved in 2011 by the FDA for the metastatic melanoma and primarily directed towards the *V600E-BRAF* mutation [5]. This has substantially increased the efficacy with a total response rate of about 48% when compared with chemotherapy which is about 5% with dacarbazine [6].

Notwithstanding these achievements, resistance development of most patients to vemurafenib [7, 8] and high rates of squamous cell carcinomas attributed to the known inhibitors and keratoacanthoma have been reported [6, 9]. Moreover, what should be mentioned is that the rate of melanoma has considerably expanded over the past decade [10, 11]. Consequently, to address the shortcomings of vemurafenib and some other related drugs, the research and development of novel effective *V600E-BRAF* kinase inhibitors are significantly relevant. In the process of drug

* Correspondence: abdallahbum@gmail.com.com
Department of Chemistry, Faculty of Physical Sciences, Ahmad Bello University, P.M.B. 1045, Zaria, Kaduna State, Nigeria

discovery, desirable lead identification is always achieved by conducting high-throughput experimental screening (HTS), but it is costly and time-consuming [12]. Hence, it is essential to overcome the limitations of traditional drug discovery approaches with effective, low-cost, and broad-spectrum modeling methods. The high-throughput computational screening, which is broadly applied presently in pharmaceutical industries, is a screening strategy generally employed by the medicinal chemist. The availability of protein crystal structures as a template for virtual screening enhances the feasibility of virtual screening [4, 13].

Furthermore, a set of thirty-one (31) potent 2-(1H-imidazol-2-yl) pyridine derivatives was synthesized and biologically evaluated for BRAF kinase inhibitory activity by Jiao et al. [14]. The reported compounds have shown remarkable biological activities against the A375 melanoma cell line. Thus, in the present investigation, these compounds were screened on *V600E-BRAF* kinase (a known melanoma target) [15] utilizing in silico molecular docking strategy to predict interactions between the compounds and the enzyme, saving money and time through the process of drug filtering. Additionally, the compounds were further screened by drug-likeness rules for oral bioavailability and pharmacokinetics ADMET (absorption, distribution, metabolism, excretion, and toxicity) properties.

Methods

Ligand selection and optimization

A series of thirty-one (31) novel 2-(1H-imidazol-2-yl) pyridine derivatives were retrieved from the literature [14]. The 2D chemical structures of the compounds were generated using ChemDraw Version 12.0 and presented in Table 1. The 2D structures were converted into the 3D structures utilizing the Spartan 14 Version 1.1.4 software package from Wavefunction Inc. The structures of the compounds were cleaned by checking and minimizing using a molecular mechanic force field (MM2) to eliminate all strain from the molecular structures. Also, this will guarantee a well-defined conformer relationship among compounds of the study [16]. The geometrical optimization of the cleansed structures was conducted with the density functional theory (DFT) at the B3LYP and 6-311G (d) basis set. The optimized molecular structures were saved in the PDB format for molecular docking and then taken to the Molegro Virtual Docker (MVD) [17], for the docking simulation purposes.

Preparation of protein and docking simulation

The X-ray structure (3D) of the protein (*V600E-BRAF*) bound with vemurafenib (PDB-ID: 3OG7) [18–20] was obtained from (http://www.rcsb.org/). The PDB file of *V600E-BRAF* was prepared with MVD [17] by removing the excess water molecules enclosed in the X-ray structure and optimizing the hydrogen molecules, and the bound vemurafenib was similarly removed from the receptor before for the docking method. The binding cavity of the *V600E-BRAF* receptor was predicted and was set inside a restricted sphere of *X*: 1.59, *Y*: − 1.28, and *Z*: −6.21 with a radius 28 Å having a grid resolution of 0.30 Å.

For the docking simulation, the prepared ligands including reference inhibitor (vemurafenib) were imported into the MVD and their bond flexibility was set collectively with the side chains of the amino acid, which was similarly set inside the defined sphere. The flexibility was set with a strength of 0.90 and a tolerance of 1.10 Å. The RMSD threshold was set as 2.00 Å for the multiple clusters poses with 100.00 energy penalty values. The docking algorithm was set for a maximum of 1500 iteration with a simplex evolution size of 50. The docking simulation was run for a minimum of 50 times for the 10 poses, and the best poses were determined based on the set scoring functions such as the MolDock score, rerank score, E-interaction, and E-H-bond [21]. Discovery Studio (DS) Visualizer Version 3.5 was utilized for the visualization of various intermolecular interactions such as H-bond, hydrophobic, halo-bond, and aryl interactions.

Drug likeness and pharmacokinetics properties prediction

The use of computational devices for identifying the novel drug candidate assists to reduce the number of experimental studies and for enhancing the success rate. For this purpose, we employed Lipinski's and Veber's rules for drug likeness as a primary screening step for oral bioavailability and synthetic accessibility using SwissADME (www.swissadme.ch/) online tool [22]. Besides, secondary screening was accompanied by calculating the ADMET properties as a measure of the pharmacokinetics [23] using pkCSM (http://biosig.unimelb.edu.au/pkcsm//) an online server.

Results

The docking result of the studied compounds against *V600E-BRAF* (PDB ID: 3OG7), exhibited that these compounds were docked at the binding site of the *V600E-BRAF* receptor with a favorable MolDock score and rerank score compared to vemurafenib (Table 2). The complete docking results and kinds of interactions associated are shown in Tables 2 and 3 respectively. Similarly, Figs. 1, 2, 3, 4, and 5 portrayed the 3D and 2D binding modes of the docked compounds at the binding cavity of V600E-BRAF. The compounds with the good MolDock score (≥ −154.482) and rerank score (≥ −116.174) were classified as potential hits (having higher binding scores than vemurafenib). Additionally, Table 4 showed the correlation analysis of the observed biological activity of the

Table 1 Chemical structures of the studied compounds

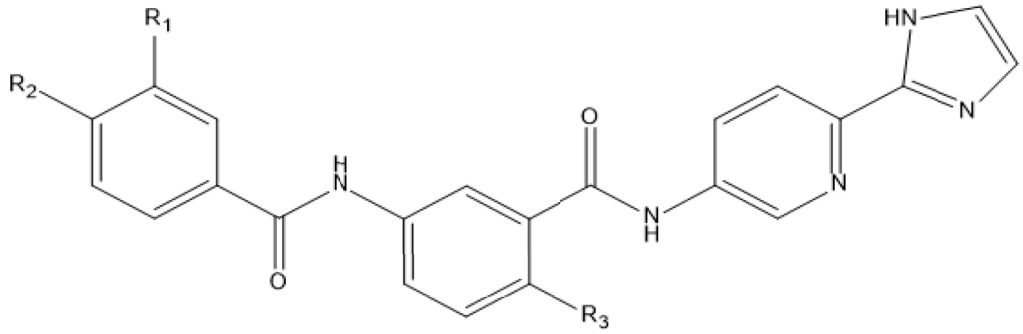

SN	R_1	R_2	R_3	SN	R_1	R_2	R_3
1	CF_3	Cl	CH_3	14	CF_3	Cl	Cl
2	CH_3	Cl	CH_3	15	CH_3	Cl	Cl
3	H	CF_3	CH_3	16	CF_3	H	Cl
4	H	CH_3	CH_3	17	H	CF_3	Cl
5	F	H	CH_3	18	CH_3	H	Cl
6	Cl	Cl	CH_3	19	H	CH3	Cl
7	OCH_3	H	CH_3	20	F	H	Cl
8	H	F	CH_3	21	Cl	H	Cl
9	H	Cl	CH_3	22	Cl	Cl	Cl
10	NO_2	H	CH_3	23	OCH_3	H	Cl
11	H	OCH_3	CH_3	24	H	F	Cl
12	Br	H	CH_3	25	H	Cl	Cl
13	H	Br	CH_3	26	Cl	Br	Cl

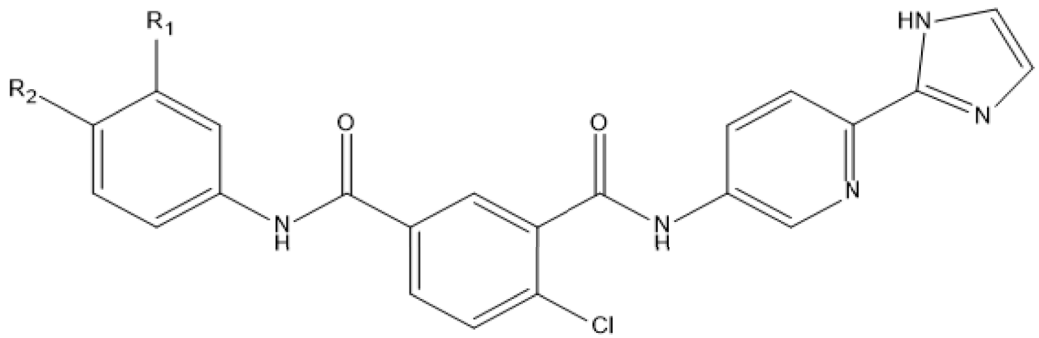

SN	R_1	R_2	SN	R_1	R_2
27	CF_3	Cl	30	Cl	H
28	CF_3	H	31	Cl	Cl
29	H	Cl			

compounds and the obtained docking results. Besides, to guarantee that the chosen compounds are the viable drugs, the drug likeness and ADMET properties were evaluated with vemurafenib as the reference. The SwissADME online tool was used to predict the drug-likeness properties as presented in Table 5, and the pkCSM online tool was adopted in predicting the ADME T properties (Table 6).

Table 2 The docking results (scores) of the studied compounds with vemurafenib as reference

Complex	MolDock score[a]	Rerank score[b]	E-interaction[c]	E-H-bond[d]	LE^1	LE^3
1	−139.825	−117.051	−163.472	−1.852	−3.995	−3.344
2	−139.934	−108.900	−148.876	−1.498	−4.373	−3.403
3	−147.450	−89.409	−158.070	−2.620	−4.337	−2.630
4	−139.765	−68.890	−145.643	−2.500	−4.509	−2.222
5	−137.994	−65.142	−150.248	−1.834	−4.451	−2.101
6	−144.459	−88.283	−151.585	−2.500	−4.514	−2.759
7	−142.277	−117.257	−149.356	−3.739	−4.446	−3.664
8	−139.488	−68.780	−154.356	−1.764	−4.500	−2.219
9	−142.525	−112.260	−151.491	−3.130	−4.598	−3.621
10	−141.901	−65.527	−157.535	−6.497	−4.300	−1.986
11	−144.286	−8.428	−156.225	−2.122	−4.509	−0.263
12	−139.632	−118.097	−158.816	−2.918	−4.504	−3.810
13	−138.905	−110.602	−155.144	−4.813	−4.481	−3.568
14	**−162.670**	**−124.079**	**−168.509**	**−3.217**	**−4.076**	**−3.545**
15	−144.133	−117.688	−152.972	−2.332	−4.504	−3.678
16	−152.301	−128.722	−172.423	−0.045	−4.479	−3.786
17	−150.734	−125.396	−162.417	−1.940	−4.433	−3.688
18	−143.411	−113.953	−151.463	−3.475	−4.626	−3.676
19	−142.213	−113.563	−150.359	−0.940	−4.588	−3.663
20	−145.590	−115.160	−153.277	−3.019	−4.696	−3.715
21	**−157.755**	**−118.218**	**−160.847**	**−2.902**	**−4.541**	**−3.684**
22	−149.608	−118.191	−160.997	−5.409	−4.675	−3.693
23	−142.708	−115.654	−152.599	−3.188	−4.460	−3.614
24	−146.940	−121.689	−161.087	−0.132	−4.740	−3.925
25	−145.794	−112.681	−158.923	−5.189	−4.703	−3.635
26	**−151.926**	**−120.707**	**−153.136**	**−3.361**	**−4.435**	**−3.585**
27	−144.135	−110.120	−166.439	−2.182	−4.118	−3.146
28	−145.964	−121.512	−158.434	−2.481	−4.293	−3.574
29	−136.121	−108.690	−142.829	−2.500	−4.391	−3.506
30	**−167.610**	**−122.290**	**−173.673**	**−3.778**	**−4.439**	**−2.655**
31	−136.246	−108.025	−144.947	−1.755	−4.258	−3.376
Vem.	**−154.482**	**−116.174**	**−164.502**	**−4.370**	**−4.681**	**−3.520**

LE^1 ligand efficiency-1 (MolDock score/heavy atoms count), LE^3 ligand efficiency 3 (rerank score/heavy atoms count)
[a]MolDock score was obtained from the PLP scoring functions with a new H-bond term and extra charge schemes [17]
[b]Rerank score is a linear combination of E-inter (electrostatic, Van der Waals, H-bonding, steric) between the ligand and the protein target, and E-intra (electrostatic, Van der Waals, H-bonding, sp2–sp2, torsion) of the ligand weighted by pre-defined coefficients [17]
[c]E-interaction is the total energy between the protein and the pose
[d]E-H-bond is H-bond energy

Discussions

The potential of the investigated compounds to interact with the receptor is presented in terms of MolDock score and rerank score respectively. The MolDock score and rerank scoring are adopted as the parameters for examining the docking results. From Table 2 (docking result), it is observed that compounds (14, 21, 26, and 30) formed bonds and non-bond interactions at the active pocket of the target as manifest from the interaction energy and H-bond energy (Table 2) and that their modes of binding (Table 3) showed some similarities to vemurafenib (standard drug), and they pose high MolDock as well as the rerank scores, this showed that the compounds had higher favorable ligand-protein E-interaction than vemurafenib at the binding pocket of the target. The docked conformations of these molecules with the lowest energy were selected for the subsequent investigations. Additionally, all the selected compounds

Table 3 Molecular interactions present in the selected complexes and the amino acids involved

Complex	Conv./pi-donor H-bond	Carbon-H-bond	Alkyl	Pi-Alkyl	Pi-pi	Pi-cation	Pi-sulfur/sigma	Halo-bond
14	LYS483 ASP594 SER536	SER535 SER535 HIS539 ASP594	ALA481 CYS532	TRP531 TRP531 HIS539 HIS539 ALA481 CYS532 LEU514 LEU505	TRP531 TRP531			GLN530 GLY534 HIS539
21	LYS483 ASP594 SER536		ALA481 LEU514 CYS532	TRP531 HIS539 ALA481 CYS532 LEU514 LEU505	TRP531			GLN530
26	LYS483 ASP594 SER536	HIS539 ASP594	ALA481 LEU514 CYS532	TRP531 HIS539 HIS539 ALA481 CYS532 LEU514 LEU505	TRP531			GLN530
30	ASP594 CYS532	GLY534	ALA481 VAL471 LYS483	PHE595 LYS483 LEU514 VAL471 ALA481 ILE463 LEU514	TRP531 PHE583 TRP531	LYS483	LEU505 CYS532	
Vem.	CYS532 ASP594 GLN530	GLY593 CYS532 THR529	LEU505 ILE527	VAL471 LYS483 ALA481 LEU514 CYS532 ALA481 CYS532	TRP531 PHE583	LYS483		ALA481

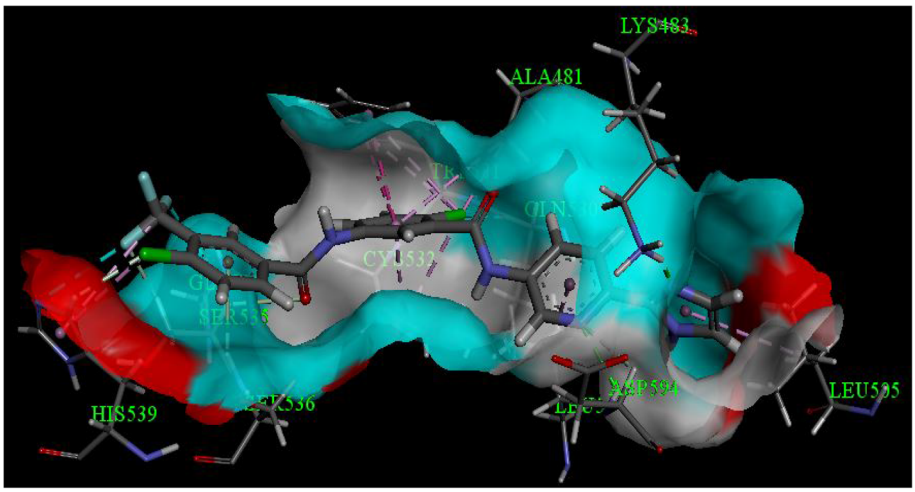

Fig. 1 3D diagram for the interaction of compound 14 with *V600E-BRAF*

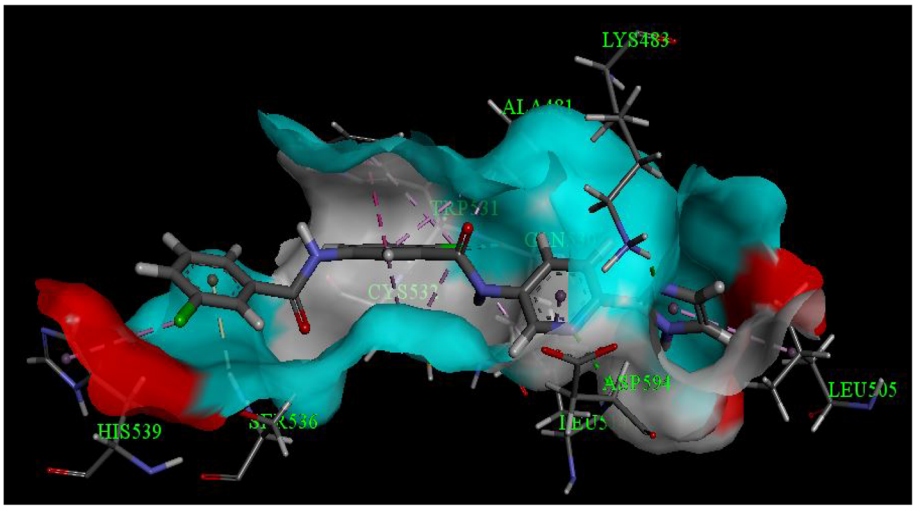

Fig. 2 3D diagram for the interaction of compound 21 with *V600E-BRAF*

have a MolDock score < −90, which indicates that the novel inhibitors can bind the target efficiently [24].

The binding mode of compound 14 and *V600E-BRAF*was depicted in Fig. 1, which has a rerank score of −124.079, and it is bonded into *V600E-BRAF*-binding cavity via two conv. hydrogen bonds, one π-donor H-bond, four carbon-H-bond, and two π-π stacked interaction. The nitrogen atom of the imidazole ring formed one H-bond with LYS483 and the other one was formed between the nitrogen atom of the pyridine ring to ASP594 residue. Two fluorine atoms of the trifluoromethyl group also formed three-carbon-H-bond with SER535 (2), HIS539, and ASP594 residues respectively. Another π-donor H-bond was observed with SER536. Moreover, the acetamido moiety is intercalated into the space to form a π-π stacked interaction with residue TRP531. There is a formation of three halogen bonds between the chlorine atom attached to the benzene ring (GLN530, GLY534, and HIS539). Besides, the higher binding score of compound 14 might also be accounted for by some weak interactions, such as alkyl with-iALA481, and CYS532, π-alkyl interaction with TRP531 (2), HIS539 (2), ALA481, CYS532, LEU514, and LEU505 residues respectively. The receptor surface model shown in Fig. 1b revealed that compound 14 has a good shape complementarity with the ATP-binding pocket of *V600E-BRAF* [25] and the abovementioned kinds of interactions may contribute to afford an explanation for its nice binding scores.

Compound 21 docked inside the active site of *V600E-BRAF* kinase (Fig. 2) revealed a better rerank score than vemurafenib (Table 2), showing that it has bound in the

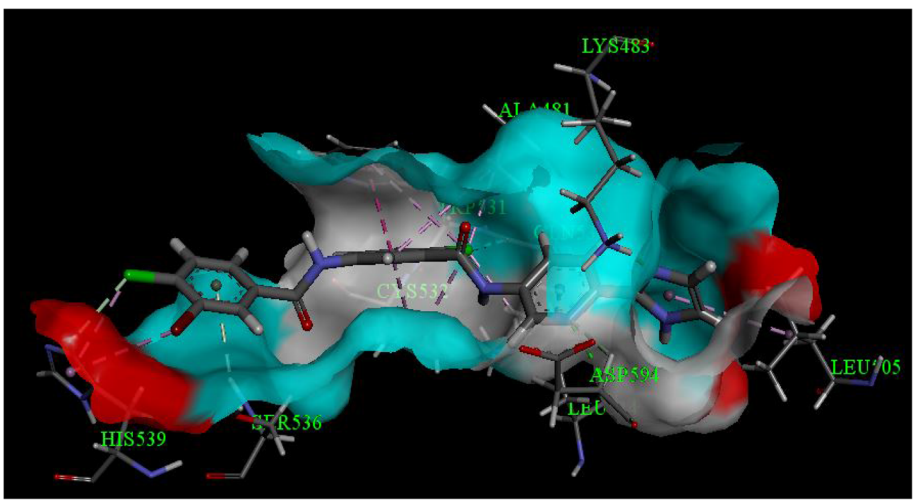

Fig. 3 3D diagram for the interaction of compound 26 with *V600E-BRAF*

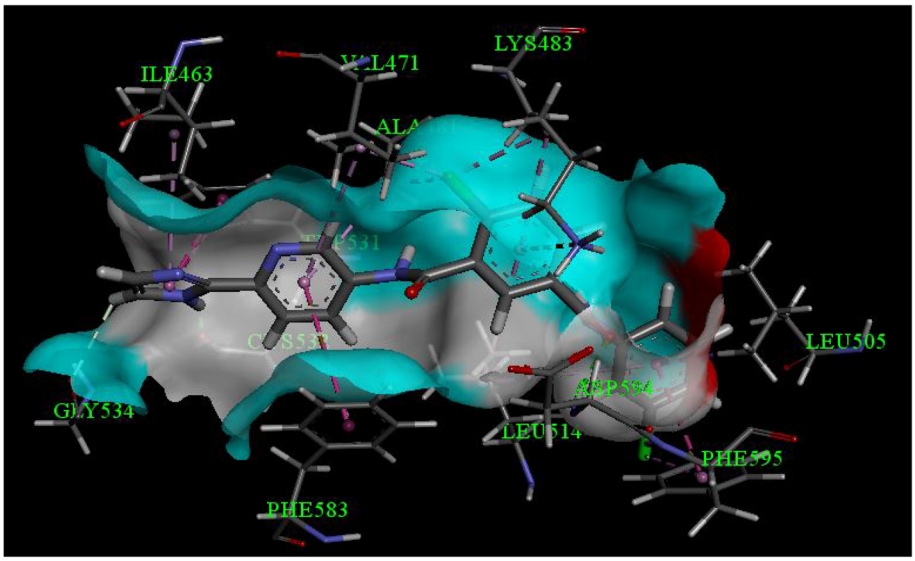

Fig. 4 3D diagram for the interaction of compound 30 with *V600E-BRAF*

active site of one of the protomers in the protein dimer through the formation of four conventional H-bond with LYS483 and ASP594 as reported in similar research [26]. The nitrogen atom of the imidazole ring formed one H-bond with LYS483 and the other one was formed between the nitrogen atom of the pyridine ring to ASP594 residue. One pi-donor H-bond was also observed with SER536 residue. There was one arene π-π interaction within the binding site and the ligand with TRP531, which befall due to the intercalation of the "benzene ring" (Fig. 2). There is a formation of one halogen bond between the fluorine atom of the triflouromethyl substituent and GLN530. There is however extra alkyl interaction with (ALA481, LEU514, and CYS532) and lastly π-alkyl interaction with six residues (TRP531, HIS539, ALA481, CYS532, LEU514, and LEU505). The results of this molecular-docking study can confirm the postulation that our active compound may inhibit the growth of melanoma cell lines through inhibition of V600E-BRAF kinase, similar to vemurafenib (Fig. 5).

The docked structure of compound 26 with the receptor is displayed in Fig. 3. It has the rerank score of −120.707, as shown in Table 2, this indicates the feasibility of good interactions that exist between this compound and the receptor. There were two conventional hydrogen bonding present between the compound and

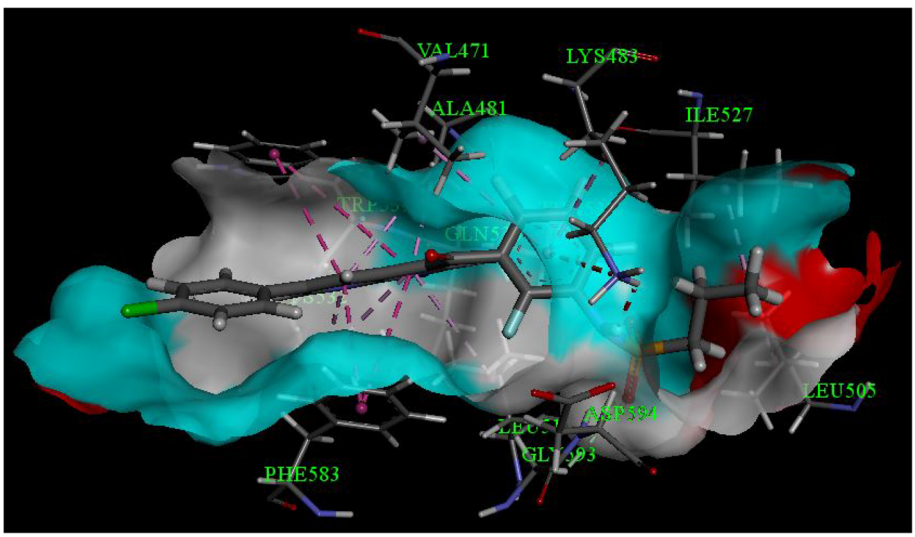

Fig. 5 3D diagram for the interaction of vemurafenib with *V600E-BRAF*

Table 4 Correlation analysis between the experimental % GI and their molecular docking studies on A375 melanoma cell line

	A375 (experimental % GI)	MolDock score[a]	Rerank score[b]	E-interaction[c]	E-H-bond[d]	LE[1]	LE[3]
A375 (experimental % GI)	1						
MolDock score[a]	−0.3429	1					
Rerank score[b]	−0.4620	0.3371	1				
E-interaction[c]	−0.4559	0.7404	0.2903	1			
E-H-bond[d]	0.1558	0.1065	−0.0346	0.0081	1		
LE[1]	0.4318	−0.0186	−0.0167	−0.2235	0.0725	1	
LE[3]	−0.3814	0.1171	0.9499	0.0769	−0.0454	0.1278	1

[a]Moldock score was obtained fromithe PLP scoring functions with ainew H-bond term and extra charge schemes [17]
[b]Rerank score is a linear combination of E-inter (Electrostatic, iVan der Waals, H-bonding, steric) between the ligand and the protein target, and E-intra. (Electrostatic, Van der Waals, H-bonding, sp2–sp2, torsion) of the ligand weighted by pre-defined coefficients [17]
[c]E-interaction is the total energy between the protein and the pose
[d]E-Hbond is Hbond energy. LE1: Ligand efficiency-1(MolDock score/heavy atoms count); LE3: Ligand efficiency 3(Rerank score/heavy atoms count)

receptor: LYS483 and ASP594 residues between the nitrogen atoms of imidazole ring formed one H-bond with LYS483 and the other one was formed between the nitrogen atoms of the pyridine ring to ASP594 residue as presented in Fig. 3. Two carbon-H-bond with HIS539 and ASP594 was also observed. There is however formation of one halogen bond with GLN530 (Fig. 3). The stability of the complex might be associated with an extra, three alkyl interaction with ALA481, LEU514, and CYS532, seven π-alkyl interactions (TRP531, HIS539 (2), ALA481, CYS532, LEU514, and LEU505 residues) plus one π-π interaction with TRP531 as reported in similar research [25].

Figure 4 showed the docked structure of compound 30 with the receptor. It presents a good rerank score of −122.290, as shown in Table 2, this exhibited the feasibility of stable interaction between this compound and the receptor. There were two conventional hydrogen bonding recognized between this compound d V600E-BRAF: ASP594 and CYS532, one pi-donor H-bond with SER536, and two carbon-H-bonds interaction with HIS539 and ASP594 residues. The π-cation interaction was formed between a benzene ring and LYS483 in a similar way to vemurafenib (Fig. 5). The benzene ring moiety has intercalated into the space to form a π-π stacked interaction with the residues (TRP531 (2) and PHE583) similar to vemurafenib (Fig. 5). The stability of the complex may be related to an extra, alkyl interaction with ALA481, VAL471, and LYS483 and π-alkyl type of interactions with PHE595, LYS483, LEU514, VAL471, ALA481, ILE463, and LEU514 residues sequentially. Comparable residues were observed for the same receptor in other literature [27].

Table 5 Drug-likeness parameters including bioavailability (BA) and synthetic accessibility (SA) of the selected compounds

Lipinski's rule					Veber's rule			
SN	Mol. wt.	HBA	HBD	Log P	NRB	TPSA (Å^2)	BA	SA
14	520.29	7	3	2.95	8	99.77	0.55	3.04
21	452.29	4	3	2.16	7	99.77	0.55	2.85
26	531.19	4	3	2.74	7	99.77	0.55	2.96
30	452.29	4	3	2.16	7	99.77	0.55	2.83
Vem.	489.92	6	2	4.97	7	100.30	0.55	3.38

Mol. wt. molecular weight, *HBA* hydrogen bond acceptor, *HDB* hydrogen bond donor, *NRB* number of rotatable bonds, *TPSA* topological polar surface area

The study showed that H-bonding is the main force controlling the interactions that exist between the docked compound and the protein target and also the interaction energy of the compounds increases with the increase in the number of the hydrogen bonds [27, 28]. It could be noted that in the conventional hydrogen bonding classified with some of the selected compounds, the number of amino acids linked was found to be better compared to vemurafenib as displayed in Figs. 1, 2, 3, 4, and 5 sequentially and there are great similarities. This might inform the more stable binding scores of the chosen compounds for *V600E-BRAF*. Thus, these compounds will serve as good inhibitors of *V600E-BRAF* showing competitive inhibition with vemurafenib as evident from the molecular-docking results.

To ensure that the chosen compounds are the viable drugs, the drug likeness, and pharmacokinetic (ADMET) properties were evaluated with vemurafenib as the reference. The SwissADME [22] online tool was used to predict the drug-likeness properties as presented in Table 5 and the pkCSM online tool was adopted in predicting the ADMET properties (Table 6). The drug-likeness parameters are the main criteria used in screening drug candidates at an initial stage of the drug discovery process. This approach can be described as a means to correlate the physicochemical properties of a given molecule with the bio-pharmaceutical aspect of it in a human body, particularly, its influence on oral bioavailability [29].

The most initial thorough investigation of drug-likeness properties was conducted by Lipinski [30] and resulted in the popular "rule of 5," which claims that good absorption or permeation is more likely when the

Table 6 Predicted the pharmacokinetic properties of the selected compounds

Absorption		Distribution			Metabolism							Excretion	Toxicity
					Substrate				Inhibitor				
					CYP								
SN	Intestinal absorption	VDss (human)	BBB permeability	CNS permeability	2D6	3A4	1A2	2C19	2C9	2D6	3A4	Total clearance	AMES toxicity
	Numeric (% absorbed)	Numeric (log L kg^{-1})	Numeric (log BB)	Numeric (log PS)				(Yes/no)				Numeric (log mL min^{-1} kg^{-1})	(Yes/no)
14	97.757	0.021	−1.735	−2.135	No	No	No	Yes	Yes	No	Yes	0.538	No
21	95.444	0.018	−1.43	−2.292	No	No	No	Yes	Yes	No	Yes	0.719	No
26	96.367	0.014	−1.614	−2.148	No	No	No	Yes	Yes	No	Yes	0.841	No
30	90.429	−0.013	−1.496	−2.295	No	No	No	Yes	Yes	No	Yes	0.667	Yes
Vem.	98.853	−0.445	−1.647	−3.463	No	Yes	No	Yes	Yes	No	Yes	0.132	No

VDss volume of distribution, *BBB* blood-brain barrier, *CNS* central nervous system, *CYP* cytochrome P

molecular weight (mol. wt.) < 500. The number of hydrogen bond donors (HBD) < 5 (counting the sum of all NH and OH groups) partition coefficient octanol/water Log *P* < 5. The number of hydrogen bond acceptors (HBA) < 10 (counting all N and O atoms). The results obtained are presented in Table 5. There are two other descriptors recognized by Veber et al. [31]: number of rotatable bonds (NRB) < 10 and polar surface area (PSA) < 140 Å2. All the chosen compounds satisfy Lipinski's and Veber's rules favorably implying that these compounds have ideal oral bioavailability. These physicochemical parameters are connected with acceptable aqueous solubility and intestinal permeability that are the first steps in oral bioavailability.

An evaluation was also performed using a bioavailability score (ABS) criteria [32], where all the compounds have 0.55 as obtained value. This criterion was based on a probability value of a molecule to have an optimum profile of permeability and bioavailability, where 0.55 indicates the obedience of the Lipinski rule of five [30] and the rat bioavailability value is 55%, which is a higher probability value than 10%. Besides, the chosen compounds were also evaluated for their synthetic accessibility, checking on a scale between 1 (very simple to synthesize) and 10 (very hard and complex to synthesize). The synthetic accessibility for all chosen compounds is around 2 to 3 (Table 5), and therefore, they are simple to synthesize.

Further, an absorbance value belowi30% indicates poor absorbance, and as observed from Table 6, all selected compounds displayed a value greater than 90%, which shows good absorbance in the human intestine. For the volume of distribution (VDss), a value > 0.45 is considered to be high. Blood-brain barrier (BBB) and the permeability of central nervous system (CNS) standard values are given as > 0.3 to < −1 log BB and > −2 to < −3ilog PS. Thus, for a given molecule, log BB < −1 indicates a poor distribution of the drug to the brain, while a value of log BB > 0.3 implies that the drug can cross the BBB. As for log PS, a value > −2 implies that the drug candidate can penetrate the CNS, while a value < −3iindicates that it will be difficult for the drug candidate to induce into the CNS [33]. The results presented in Table 6, indicated that the selected compounds have shown a high potential to cross barriers.

The metabolism describes the biochemical transformation of a drug candidate by the body. Consequently, drugs usually give several metabolites, which might have different pharmacological and physicochemical properties. It is necessary to consider the metabolism of the drugs and drug-drug interactions [34]. The CYP450 (cytochromeiP450) plays a vital role in drug metabolism because it is the main liver protein system involved in oxidation (phase-1 metabolism), as in the case of this research. To date, only 17 CYP families were identified in humans, even though only CYP1, CYP2, CYP3, and CYP4, sequentially) are involved in the drug metabolism, with a CYP (1A2, 2C9, 2C19, 2D6 and 3A4, respectively) were identified to be responsible for the biotransformation of more than 90% of the drugs that undergo phase-I metabolism [34, 35] and have been predicted and presented in Table 6.iAdditionally, cytochrome CYP3A4 inhibition is the most vital phenomenon in this research [36]. The results presented in Table 6, indicated that all the selected compounds are the inhibitors of 2C19, 2C9, and CYP3A4 respectively.

Clearance describes the relationship of the drug concentration in the body to the rate of its elimination. Thus, a lower value of the total clearance implies increased persistence of the drugs in the human body, and all the selected compounds showed good persistence in the body for the drug. Additionally, it is required to investigate whether the selected compounds are nontoxic as this plays a significant role in selecting the best drugs. The results presented in Table 6, indicated that compounds 14, 21, and 26 are nontoxic. All the selected compounds displayed good physicochemical and

pharmacokinetic ADMET properties. Thus, based on these results, it can be presumed that these compounds can be adopted as V600E-BRAF inhibitors and drugs on melanoma cancer in the future.

Conclusion

*V600E-BRAF*is a vital and attractive therapeutic enzyme in melanoma and other types of cancer. Nevertheless, its acquired resistance to vemurafenib and side effects of some other drugs in several events has been published. Therefore, to further explore the anti-proliferative potential of V600E-BRAF inhibitors, we applied docking virtual screening joined with an in silico drug likeness and ADMET evaluations to screen a series of potent 2-(1H-imidazol-2-yl) pyridine derivatives. A total of four analogs of 2-(1H-imidazol-2-yl) pyridine derivatives (14, 21, 26, and 30) exhibited favorable interaction and a more reliable binding score than vemurafenib, exhibiting common molecular interaction with CYS532, ASP594, TRP531, and PHE583 residues of *V600E-BRAF*. Besides, the compounds employed in this study do not violate the Lipinski's and Veber's rules for drug likeness to qualify as orally active drugs and the ADMET evaluation shows that they are pharmacologically active. These could be likely used as lead compounds with improved pharmacological properties.

Abbreviations

DFT: Density functional theory; MVD: Molegro virtual docker; ADMET: Absorption, distribution, metabolism, excretion, and toxicity; HBD: Hydrogen bond donor; HBA: Hydrogen bond acceptor

Acknowledgements

The authors acknowledge the Ahmadu Bello University, Zaria-Nigeria for the technical support and all the members of the Physical Chemistry Research Group for their kind advice and encouragement.

Authors' contributions

AU designed the study. ABU carried out docking simulation, drug likeness, and ADMET properties predictions and drafted the manuscript. GAS and SU participated in designing the study and edited the manuscript. All authors read and approved the final manuscript.

Funding

Not applicable.

Availability of data and materials

All data generated or analyzed during this study are included in this published article.

Ethics approval and consent to participate

Not applicable.

Consent for publication

Not applicable.

Competing interests

The authors declare that they have no competing interests.

Received: 19 August 2020 Accepted: 10 November 2020
Published online: 30 November 2020

References

1. Li Z, Jiang J-D, Kong W-J (2014) Berberine up-regulates hepatic low-density lipoprotein receptor through Ras-independent but AMP-activated protein kinase-dependent Raf-1 activation. Biol Pharm Bull 37(11):1766–1775
2. Holderfield M, Deuker MM, McCormick F, McMahon M (2014) Targeting RAF kinases for cancer therapy: BRAF-mutated melanoma and beyond. Nat Rev Cancer 14(7):455–467
3. Villanueva J, Vultur A, Lee JT, Somasundaram R, Fukunaga-Kalabis M, Cipolla AK, Wubbenhorst B, Xu X, Gimotty PA, Kee D (2010) Acquired resistance to BRAF inhibitors mediated by a RAF kinase switch in melanoma can be overcome by cotargeting MEK and IGF-1R/PI3K. Cancer Cell 18(6):683–695
4. Luo C, Xie P, Marmorstein R (2008) Identification of BRAF inhibitors through in silico screening. J Med Chem 51(19):6121–6127
5. Robinson SD, O'Shaughnessy JA, Cowey CL, Konduri K (2014) BRAF V600E-mutated lung adenocarcinoma with metastases to the brain responding to treatment with vemurafenib. Lung Cancer 85(2):326–330
6. Chapman PB, Hauschild A, Robert C, Haanen JB, Ascierto P, Larkin J, Dummer R, Garbe C, Testori A, Maio M (2011) Improved survival with vemurafenib in melanoma with BRAF V600E mutation. N Engl J Med 364(26):2507–2516
7. Zhan Y, Dahabieh MS, Rajakumar A, Dobocan MC, M'Boutchou M-N, Goncalves C, Lucy SL, Pettersson F, Topisirovic I, van Kempen L (2015) The role of eIF4E in response and acquired resistance to vemurafenib in melanoma. J Investig Dermato 135(5):1368–1376
8. Liu F, Cao J, Wu J, Sullivan K, Shen J, Ryu B, Xu Z, Wei W, Cui R (2013) Stat3-targeted therapies overcome the acquired resistance to vemurafenib in melanomas. J Investig Dermato 133(8):2041–2049
9. Martinez-Garcia M, Banerji U, Albanell J, Bahleda R, Dolly S, Kraeber-Bodéré F, Rojo F, Routier E, Guarin E, Xu Z-X (2012) First-in-human, phase I dose-escalation study of the safety, pharmacokinetics, and pharmacodynamics of RO5126766, a first-in-class dual MEK/RAF inhibitor in patients with solid tumors. Clin Cancer Res 18(17):4806–4819
10. Helvind NM, Hölmich LR, Smith S, Glud M, Andersen KK, Dalton SO, Drzewiecki KT (2015) Incidence of in situ and invasive melanoma in Denmark from 1985 through 2012: a national database study of 24 059 melanoma cases. JAMA Dermatol 151(10):1087–1095
11. Barbaric J, Sekerija M, Agius D, Coza D, Dimitrova N, Demetriou A, Diba CS, Eser S, Gavric Z, Primic-Zakelj M (2016) Disparities in melanoma incidence and mortality in South-Eastern Europe: increasing incidence and divergent mortality patterns. Is progress around the corner? Eur J Cancer 55:47–55
12. Cheng T, Li Q, Zhou Z, Wang Y, Bryant SH (2012) Structure-based virtual screening for drug discovery: a problem-centric review. AAPS J 14(1):133–141
13. Schmidt T, Bergner A, Schwede T (2014) Modelling three-dimensional protein structures for applications in drug design. Drug Discov Today 19(7):890–897
14. Jiao Y, Xin B-T, Zhang Y, Wu J, Lu X, Zheng Y, Tang W, Zhou X (2015) Design, synthesis and evaluation of novel 2-(1H-imidazol-2-yl) pyridine Sorafenib derivatives as potential BRAF inhibitors and anti-tumor agents. Eur J Med Chem 90:170–183
15. Dhillon AS, Hagan S, Rath O, Kolch W (2007) MAP kinase signalling pathways in cancer. Oncogene. 26(22):3279
16. Ulrich B, Norman L (1982) Molecular mechanics (ACS monograph 177). Am Chem Soc, Washington, DC
17. Molegro A (2011) MVD 5.0 Molegro Virtual Docker. DK-8000 Aarhus C, Denmark
18. Brose MS, Volpe P, Feldman M, Kumar M, Rishi I, Gerrero R, Einhorn E, Herlyn M, Minna J, Nicholson A (2002) BRAF and RAS mutations in human lung cancer and melanoma. Cancer Res 62(23):6997–7000
19. Bollag G, Hirth P, Tsai J, Zhang J, Ibrahim PN, Cho H, Spevak W, Zhang C, Zhang Y, Habets G (2010) Clinical efficacy of a RAF inhibitor needs broad target blockade in BRAF-mutant melanoma. Nature. 467(7315):596
20. Choi W-K, El-Gamal MI, Choi HS, Baek D, Oh C-H (2011) New diarylureas and diarylamides containing 1, 3, 4-triarylpyrazole scaffold: synthesis, antiproliferative evaluation against melanoma cell lines, ERK kinase inhibition, and molecular docking studies. Eur J Med Chem 46(12):5754–5762
21. Thomsen R, Christensen MH (2006) MolDock: a new technique for high-accuracy molecular docking. J Med Chem 49(11):3315–3321

22. Daina A, Michielin O, Zoete V (2017) SwissADME: a free web tool to evaluate pharmacokinetics, drug-likeness and medicinal chemistry friendliness of small molecules. Sci Rep 7:42717
23. Martinez-Mayorga K, Madariaga-Mazon A, Medina-Franco JL, Maggiora G (2020) The impact of chemoinformatics on drug discovery in the pharmaceutical industry. Expert Opin Drug Discovery 15(3):293–306
24. Abdullahi M, Uzairu A, Shallangwa GA, Arthur DE, Umar BA, Ibrahim MT (2020) Virtual molecular docking study of some novel carboxamide series as new anti-tubercular agents. Eur J Chem 11(1):30–36
25. Umar AB, Uzairu A, Shallangwa GA, Uba S (2020) In silico evaluation of some 4-(quinolin-2-yl) pyrimidin-2-amine derivatives as potent V600E-BRAF inhibitors with pharmacokinetics ADMET and drug-likeness predictions. Fut J Pharmaceut Sci 6(1):1–10
26. Umar AB, Uzairu A, Shallangwa GA, Uba S (2020) QSAR modelling and molecular docking studies for anti-cancer compounds against melanoma cell line SK-MEL-2. Heliyon. 6(3):e03640
27. Umar BA, Uzairu A, Shallangwa GA, Uba S (2019) Rational drug design of potent V600E-BRAF kinase inhibitors through molecular docking simulation. J Eng Exact Sci 5(5):0469–0481
28. Adedirin O, Uzairu A, Shallangwa GA, Abechi SE (2018) Optimization of the anticonvulsant activity of 2-acetamido-N-benzyl-2-(5-methylfuran-2-yl) acetamide using QSAR modeling and molecular docking techniques. Beni-Suef Univ J Basic Appl Sci 7(4):430–440
29. Bickerton GR, Paolini GV, Besnard J, Muresan S, Hopkins AL (2012) Quantifying the chemical beauty of drugs. Nat Chem 4(2):90
30. Lipinski CA, Lombardo F, Dominy BW, Feeney PJ (1997) Experimental and computational approaches to estimate solubility and permeability in drug discovery and development settings. Adv Drug Deliv Rev 23(1-3):3–25
31. Veber DF, Johnson SR, Cheng H-Y, Smith BR, Ward KW, Kopple KD (2002) Molecular properties that influence the oral bioavailability of drug candidates. J Med Chem 45(12):2615–2623
32. Martin YC (2005) A bioavailability score. J Med Chem 48(9):3164–3170
33. Clark DE (2003) In silico prediction of blood–brain barrier permeation. Drug Discov Today 8(20):927–933
34. Kok-Yong S and Lawrence L (2015) Drug distribution and drug elimination. Basic pharmacokinetic concepts and some clinical applications. TA Ahmed. Rijeka, InTech. 99-116.
35. Šrejber M, Navrátilová V, Paloncýová M, Bazgier V, Berka K, Anzenbacher P, Otyepka M (2018) Membrane-attached mammalian cytochromes P450: an overview of the membrane's effects on structure, drug binding, and interactions with redox partners. J Inorg Biochem 183:117–136
36. Thapar MM, Ashton M, Lindegårdh N, Bergqvist Y, Nivelius S, Johansson I, Björkman A (2004) Time-dependent pharmacokinetics and drug metabolism of atovaquone plus proguanil (Malarone) when taken as chemoprophylaxis. European J Clin Pharm 58(1):19–27

Publisher's Note